ACS APPLIED MATERIALS & INTERFACES

Research Article

www.acsami.org

Amphiphilic Colloidal Surfactants Based on Electrohydrodynamic Co-jetting

Jaewon Yoon,[†] Arun Kota,[‡] Srijanani Bhaskar,[†] Anish Tuteja,[‡] and Joerg Lahann*[,†,§]

[†]Department of Macromolecular Science and Engineering University of Michigan, Ann Arbor, Michigan 48109, United States of America

[‡]Department of Materials Science and Engineering University of Michigan, Ann Arbor, Michigan 48109, United States of America

[§]Departments of Chemical Engineering, Materials Science and Engineering and Biomedical Engineering University of Michigan, Ann Arbor, Michigan 48109, United States of America

Supporting Information

ABSTRACT: A novel synthetic route for the preparation of amphiphilic Janus particles based on electrohydrodynamic cojetting has been developed. In this approach, selective encapsulation of hydrophobic fluorodecyl-polyhedral oligomeric silsesquioxane (F-POSS) in one compartment and a poly(vinyl alcohol) in the second compartment results in colloidal particles with surfactant-like properties including the self-organization at oil−water and air−water interfaces. Successful localization of the respective polymers in different compartments of the same particle is confirmed by a combination of fluorescence microscopy, vibrational spectroscopy, and ζ-potential measurements. We believe that this straightforward synthetic approach may lead to a diverse class of surface-active colloids that will have significant relevance ranging from basic scientific studies to immediate applications in areas, such as pharmaceutical sciences or cosmetics.

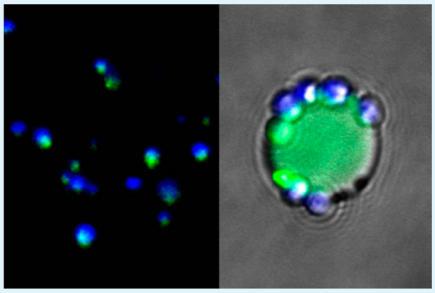

KEYWORDS: *electrohydrodynamic cojetting, amphiphilic particles, polymers*

1. INTRODUCTION

Janus particles, that is, particles displaying two regions of distinct properties, have been widely studied because of their extensive range of potential applications.[1−14] For example, Janus particles are important for colloidal formulations,[1−4] therapeutic delivery,[5−7] imaging,[8] sensing materials,[9] display devices,[10,11] or catalysts.[12−14] Unlike their isotropic counterparts, Janus particles have the potential to display different types of chemistries on different hemispheres.[15−17] Binks and co-workers compared the assembly of various particles on liquid−liquid interfaces. Their theoretical studies suggest that "Janus" particle assemblies have a higher stability upon adsorption to liquid−liquid interfaces than isotropic particles.[18] This was attributed to the surfactant-like amphiphilicity of Janus particles. In addition, there have been studies emphasizing the role of different shapes on the self-assembly of amphiphilic Janus particles.[3,19] At this point, further progress in the field is, at least in parts, hampered by the lack of suitable synthesis routes, which allow for precise engineering of critical particle properties, such as the chemical nature and geometric distribution of surface patches or the range of different materials combinations that can be presented on the individual compartments.[20]

In this work, we report a novel type of amphiphilic Janus particles with precisely tailored interfacial properties based on electrohydrodynamic (EHD) cojetting.[21,22] In the past, this method has been used to create micrometer to nanoscale particles and fibers displaying independent control over bulk properties as well as surface functionalities of the particles.[6,23] Specifically, we report colloidal particles that are comprised of hydrophilic as well as superhydrophobic interfacial regions. While the hydrophilic compartment was comprised of a poly(vinyl alcohol), highly fluorinated fluorodecyl-polyhedral oligomeric silsesquioxane (F-POSS) was selectively loaded into a second compartment to impart overall amphiphilicity. F-POSS is known to form superhydrophobic surfaces when deposited as thin films, owing to its extremely low surface energy.[24,25] However, due to the limitations in selecting solvents in which it is soluble, such molecules are difficult to process into Janus particles. EHD cojetting fulfills the need for independent control of the two compartments and allows molecules with different properties to be placed in separate compartments. To ensure stable cojetting, the first compartment was initially comprised of poly(vinyl acetate) (PVAc). PVAc was used as a precursor, which, after hydrolysis of the particle surface, was converted, in parts, into the polar poly(vinyl alcohol). The appropriate balance of hydrophilic and hydrophobic interfacial domains resulted in colloidal particles with surfactant-like properties, such as spontaneous self-assembly at liquid−air and liquid−liquid interfaces.

Received: August 21, 2013
Accepted: October 10, 2013
Published: October 10, 2013

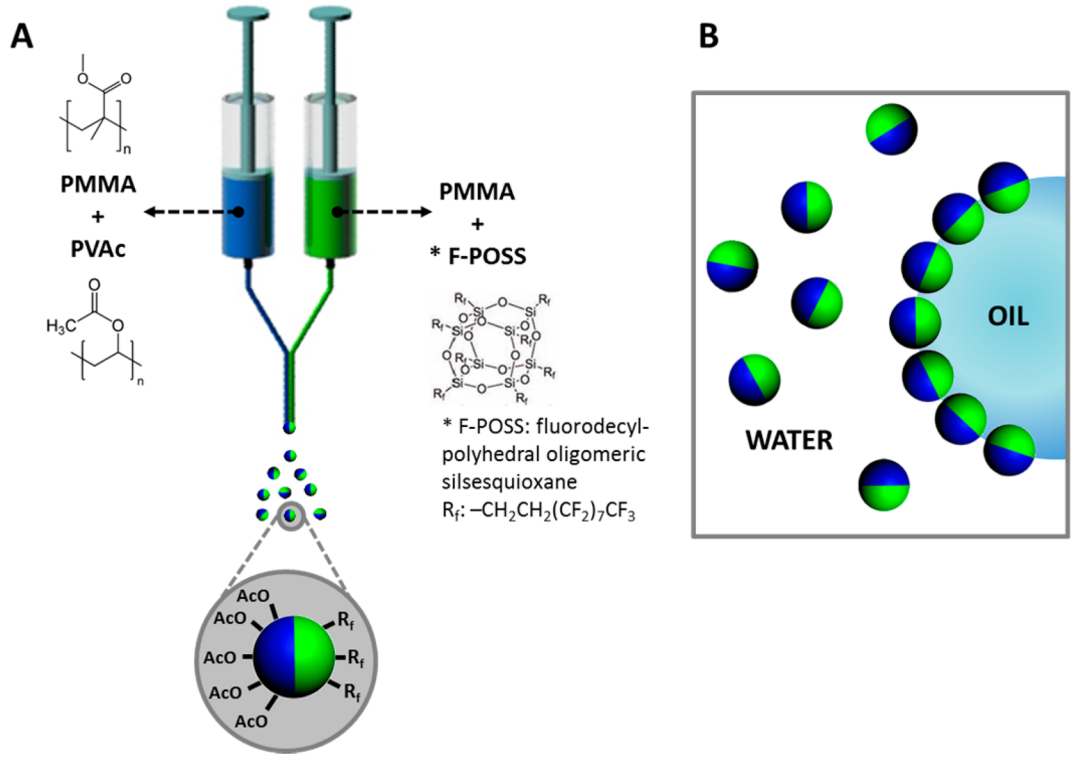

Figure 1. Fabrication of bicompartmental PMMA particles with PVAc and F-POSS in each compartment via EHD cojetting (A) and their projected self-organization at a liquid–liquid interface (B).

2. RESULTS AND DISCUSSION

Conceptionally, the herein developed synthetic route toward amphiphilic colloids was inspired by our previous work on the EHD cojetting of polymer solutions.[21] The bicompartmental character of these particles has been clearly established in a range of different particle systems. By processing two or more parallel polymer solutions with distinct chemical composition through electrified capillaries, solid particles with multiple distinct compartments can be prepared.[21] As outlined in Figure 1A, we selected a rather conventional polymer, poly(methyl methacrylate) (PMMA), as the base polymer for all amphiphilic polymer particles that were prepared in this work. PMMA is a widely used polymer because of its good solubility in common solvents and easy processing.[26−28] While both solutions contained PMMA as the major polymer component, two different functional additives, either F-POSS or PVAc, were incorporated into the respective jetting solutions to introduce different interfacial functionalities. The addition of highly fluorinated F-POSS is a probate mean to impart super-hydrophobicity to the surfaces of polymer blends, because it has been well-established that the POSS additives tend to migrate to the surface of the blend due to phase separation between two components.[24,29,30] To induce amphiphilicity, the second compartment was comprised of a blend of PVAc and PMMA. While PVAc is sufficiently apolar to be compatible with the solvents used for preparing the jetting solutions, this polymer can easily be converted into a hydrophilic polymer (i.e., PVA) after particle preparation. Simple base-catalyzed hydrolysis of interfacial acetate groups leads to hydrophilic PVA segments on the particle surface.

To achieve selective encapsulation of F-POSS and PVAc in the respective PMMA compartment, various jetting parameters had to be considered, including polymer concentration, solvent, and flow rate. As we aimed at producing microparticles, the jetting solutions were prepared at relatively low polymer concentrations (3 w/v %). The intrinsic problem of using F-POSS as an additive is its limited solubility in common organic solvents. In fact, such fluorinated compounds tend to dissolve preferentially in fluorinated solvents, and their low dielectric constants make them difficult to be processed by EHD cojetting.[25] Thus, once PMMA was selected as the base polymer, it was important to identify an appropriate solvent system. While the majority of solvents used for PMMA are comprised of THF and DMF, which were chosen to provide uniform particle shapes, a small amount of fluorinated solvent (AK-225, 5 vol% of total solvents) had to be added to dissolve the F-POSS. Hence, the hydrofluorocarbon (AK-225) was mixed with organic solvents (THF:DMF:AK-225 = 50:45:5) and two different jetting solutions—one containing PMMA/POSS and the second containing PMMA/PVAc—were separately transferred through adjacent capillaries at a constant flow rate of 0.1 mL/h. When a voltage of 6 kV was applied, the droplet which was formed at the end tip of capillaries started to eject to create highly uniform bicompartmental particles.

After synthesis, the Janus character of the particles was confirmed via direct visualization. Confocal laser scanning microscopy CLSM) has been previously established as a versatile technique to demonstrate the multicompartmental character of particles and fibers.[31,−33] For the CLSM analysis, fluorescent dyes were added to the two different jetting solutions, which have been proved to be an efficient method to index each compartment.[22,23] The combination of blue and green dyes enabled subsequent differentiation between the compartments of the as-jetted particles by CLSM. The CLSM images demonstrate the successful preparation of bicompartmental particles as indicated by the confinement of blue

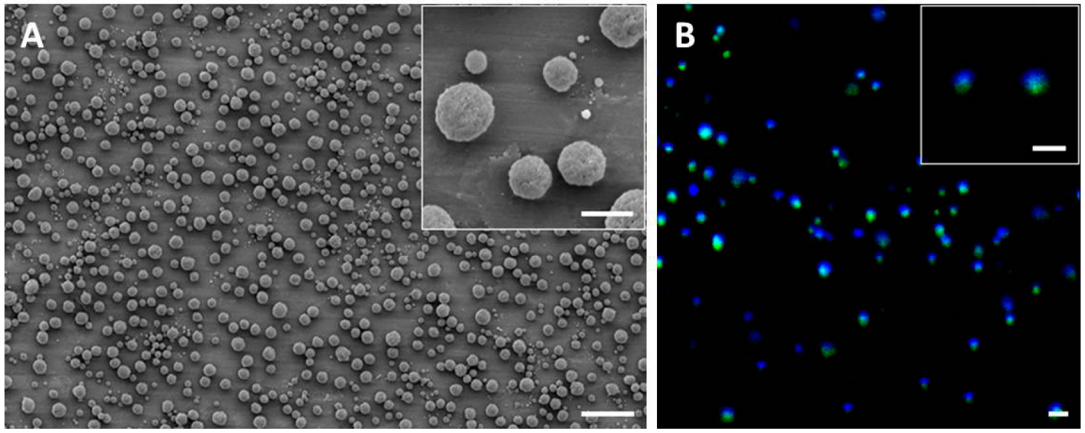

Figure 2. SEM (A) and CLSM (B) images of bicompartmental PMMA particles directly after preparation. Two additives, PVAc or F-POSS, were confined in two different hemispheres. The compartments were labeled with blue and green fluorescent dyes for the visualization. (Scale bars in A and B are 10 and 2 μm, respectively. All scale bars of the insets are 2 μm.)

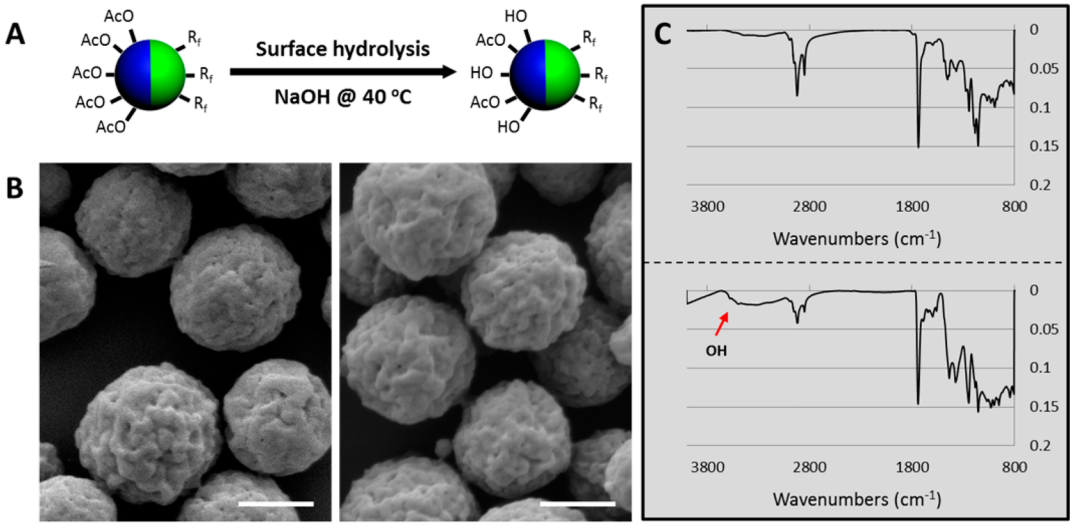

Figure 3. Surface modification of bicompartmental PMMA particles. (A) Surface hydrolysis of PVAc to PVA under basic conditions. Selective hydrolysis of the PVAc (blue) compartment renders this hemisphere hydrophilic. (B) SEM images of the particles before (left) and after (right) hydrolysis show no changes in particle morphology, which indicates that the reaction was restricted to the particle surfaces. Scale bars are all 1 μm. (C) FT-IR spectra of the corresponding particles before (top) and after (bottom) hydrolysis.

(PMMA/PVAc) and green (PMMA/F-POSS) fluorescent dyes within distinct compartments of the same particles (Figure 2B). In this case, the successful compartmentalization of micro- and nanoparticles is in good agreement with previously found results.[34,35]

For these Janus particles to exhibit amphiphilic properties, the compartmentalization of the additives is a necessary, but not sufficient prerequisite. In addition, the surface-active additives will have to be selectively present at the surface of the representative hemispheres. In the case of the highly fluorinated F-POSS, previous work already showed that F-POSS migrates onto the surface of particles.[24] Here, we confirmed a similar behavior in the blend of PMMA and F-POSS in model studies with thin polymer films. For this purpose, the same polymer blend used for electrohydrodynamic cojetting was spin-casted. The surface topography was directly observed through atomic force microscopy (AFM) to identify POSS domains. Additionally, contact angle measurements of the film were performed to confirm the presence of the POSS molecules on the surface.[24]

Second, to unambiguously confirm the presence of polar hydroxyl groups in the second compartment (PVA/PVAc), control particles were prepared by EHD cojetting. The acetate groups were partially hydrolyzed to yield partially protected poly(vinyl alcohol) (PVA) (Figure 3A). While increasing the hydroxyl groups on the hemisphere surface promotes hydrophilicity, it is important to perform the hydrolysis reaction under mild conditions. This is to prevent full deprotection of PVAc, which will render the polymer water-soluble and can result in complete dissolution, leaving behind the more hydrophobic PMMA. As shown in Figure 3B, particle morphologies were still maintained after hydrolysis indicating that the hydrolysis of PVAc was restricted to the surface, and did not occur throughout the entire bulk. The presence of hydroxyl groups on the particle surface was further demonstrated by ζ-potential measurements and FT-IR spectroscopy. Figure 3C shows FT-IR spectra of particles before and after surface hydrolysis of PVAc. The increase in the intensity of characteristic bands of OH groups near 3300 cm^{-1} indicates partial hydrolysis of acetate groups to hydroxyl groups.

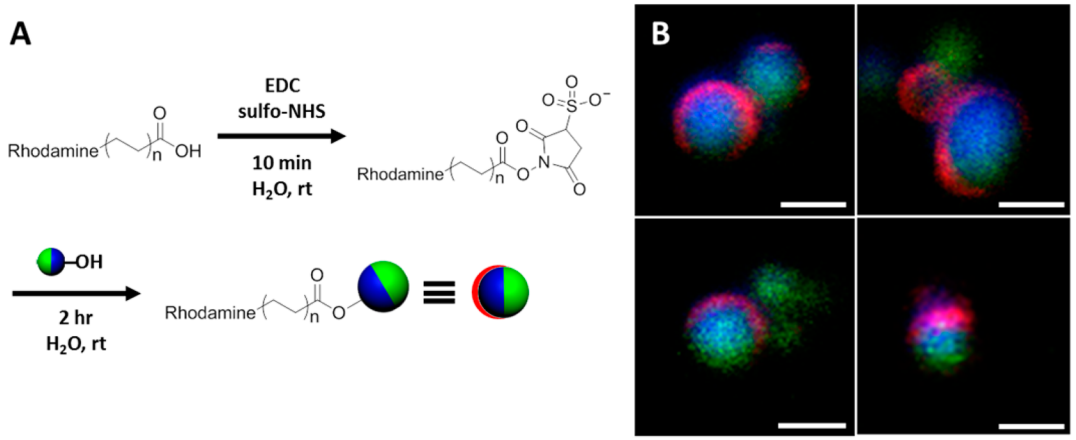

Figure 4. Presence of hydroxyl groups on the particle surface was confirmed by EDC/NHS coupling. (A) Reaction scheme; (B) CLSM images of selective conjugation of rhodamine on the particles. Scale bars are 1 μm in all images.

Additionally, ζ-potential measurements of the particles were conducted. Although the ζ-potential of the particles was an indirect method to confirm the presence of the OH groups, and taken alone are not sufficient to unambiguously confirm their presence on the surface, the values further support the results obtained from the FT-IR analysis. The ζ-potential of the particles before the hydrolysis of PVAc was +0.05 mV suggesting acrylate and acetyl groups, which are with neutral charge. After conversion of PVAc to PVA, the ζ-potential values decreased to −18.3 mV. The negative surface charge can be attributed to the dissociation of protons from hydroxyl groups created by surface hydrolysis. Thus, as the particles became hydrolyzed, the hydroxyl contents increased, yielding a more negatively charged surface. Finally, the distribution of hydroxyl groups on the particle surfaces was explicitly demonstrated by conjugation of a carboxylic acid-terminated fluorescent probe to free interfacial hydroxyl groups. For this purpose, rhodamine-PEG-carboxlic acid was activated using 1-ethyl-3-(3-dimethylaminopropyl) carbodiimide hydrochloride (EDC) and N-hydroxysulfo-succinimide sodium salt (NHS, Figure 4A). After the reaction, the resulting rhodamine-conjugated particles were characterized by CLSM (Figure 4B and C). Red fluorescence was restricted to the PMMA/PVA compartment, which was encoded with a blue dye. No overlay of red fluorescence with the green fluorescence of the PMMA/POSS compartment was observed indicating successful confinement of the hydroxyl groups to one hemisphere only.

In order to quantify the degree of hydrophilicity and hydrophobicity of our Janus particles, we estimated the surface energy using the Owens−Wendt approach.[36] According to this approach, the solid surface energy is the sum of contributions from two types of intermolecular forces at the surface:

$$\gamma_{sv} = \gamma_{sv}^{d} + \gamma_{sv}^{p} \tag{1}$$

Here, γ_{sv}^{d} is the component that accounts for the dispersive forces, while γ_{sv}^{p} is the component that accounts for the polar forces. Further, this approach postulates that

$$\gamma_{sl} = \gamma_{sv} + \gamma_{lv} - 2\sqrt{\gamma_{sv}^{d}\gamma_{lv}^{d}} - 2\sqrt{\gamma_{sv}^{p}\gamma_{lv}^{p}} \tag{2}$$

Here, γ_{lv}^{d} and γ_{lv}^{p} are the dispersive and polar components of the liquid surface tension, respectively. Combining eqs 1 and 2 with Young's equation[37] and recognizing that the polar component of liquid surface tension is zero ($\gamma_{lv}^{p} = 0$) for nonpolar liquids such as oils, the dispersive component of solid surface energy is given as

$$\gamma_{sv}^{d} = \gamma_{lv}\left(\frac{1 + \cos\theta}{2}\right)^{2} \tag{3}$$

In eq 3, γ_{lv} is the surface tension of a nonpolar liquid and θ is the equilibrium contact angle of the same nonpolar liquid on the solid surface. We used hexadecane (γ_{lv} = 27.5 mN/m)[38] as the nonpolar liquid to estimate γ_{sv}^{d}. After determining the dispersive component γ_{sv}^{d}, combining eqs 1 and 2 with Young's equation[32] for a polar liquid ($\gamma_{lv}^{p} \neq 0$), the polar component of the solid surface energy is given as

$$\gamma_{sv}^{p} = \frac{1}{\gamma_{lv}^{p}}\left[\frac{\gamma_{lv}(1 + \cos\theta)}{2} - \sqrt{\gamma_{sv}^{d}\gamma_{lv}^{d}}\right]^{2} \tag{4}$$

In eq 4, γ_{lv} is the surface tension of a polar liquid and θ is the equilibrium contact angle for the same polar liquid on the solid surface. We used water (γ_{lv}^{d} = 21.1 mN/m and γ_{lv}^{p} = 51.0 mN/m)[38] as the polar liquid to estimate γ_{sv}^{p}.

Table 1 summarizes the solid surface energy values estimated by the Owens−Wendt approach. These values were obtained by measuring the advancing contact angles (θ_{adv}) for hexadecane and water on substrates spin-coated with blends of PMMA + fluorodecyl POSS and PMMA + PVAc (both before and after hydrolysis). The PMMA + fluorodecyl POSS blend possesses a low solid surface energy with a predominant

Table 1. Estimated Dispersive Component, Polar Component, and the Total Surface Energy for Blends of PMMA + F-POSS and PMMA + PVAc (Both before and after Hydrolysis)

	θ_{adv} (water) [deg]	θ_{adv} (hexadecane) [deg]	γ_{sv}^{d} [mN/m]	γ_{sv}^{p} [mN/m]	γ_{sv} [mN/m]
PMMA + F-POSS	120 ± 2	76 ± 2	10.6	0.2	10.8
PMMA + PVAc before hydrolysis	83 ± 4	19 ± 2	26.1	5.8	31.9
PMMA + PVAc after hydrolysis	73 ± 4	17 ± 2	26.3	10.2	36.5

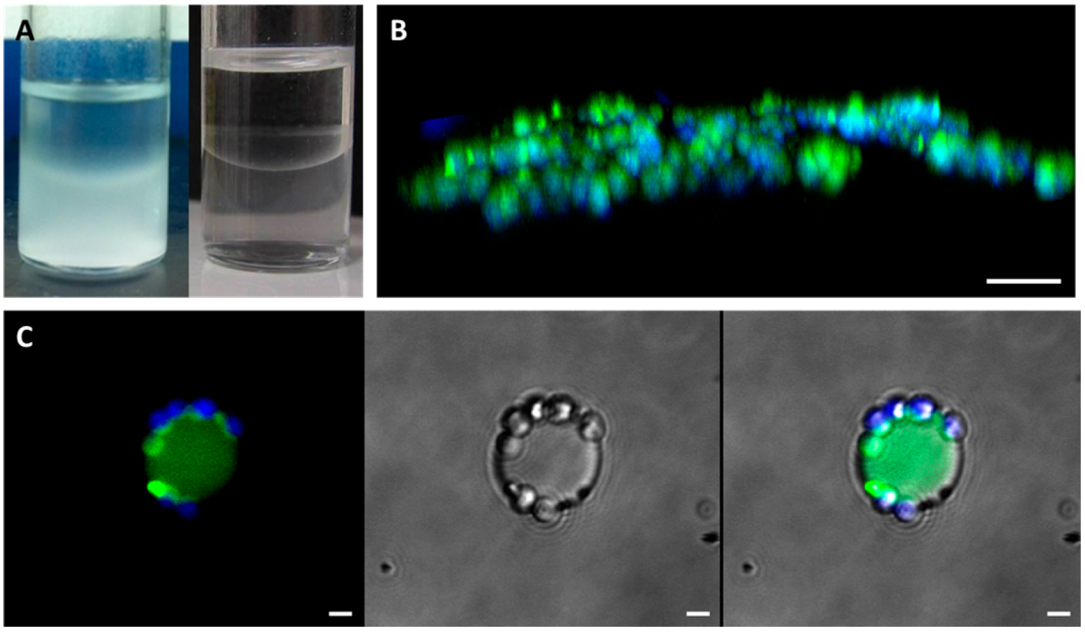

Figure 5. Oriented self-organization of particles at liquid–liquid interfaces. (A) Comparison of monophasic PMMA (left) and amphiphilic PMMA (right) particles, placed at a heptane–water interface. The images clearly show that the amphiphilic particles were self-assembled at the interface. (B) CLSM image of the orientation of these amphiphilic PMMA particles at the interface. 3D reconstruction of self-assembled particle layer shows apolar compartment (green) directing oil phase, while polar compartment (blue) facing water. (C) Adsorption of the same particles self-assembled around hexadecane droplet in water. The fluorescence image (left) and differential interference contrast (DIC) micrograph are overlaid (right).

dispersive component. This renders the surface of PMMA + fluorodecyl POSS blend hydrophobic. In comparison, the PMMA + PVAc blend before hydrolysis possesses a higher surface energy with a higher polar component. Consequently, the surface of the PMMA + PVAc blend before hydrolysis is relatively more hydrophilic compared to the surface of the PMMA + F-POSS blend. Upon hydrolysis, the polar component of surface energy for PMMA + PVAc blend increases further, thereby increasing its hydrophilicity.

Although it is difficult to measure contact angles of a particle at a liquid–liquid interface, the water contact angle measurements of the polymer films can be a reliable evidence to demonstrate wetting behaviors of each polymer compositions. The approach introduced here not only reveals the amphiphilic character of the particles, but also signifies the ways to characterize the detachment energy of the particles at the liquid–liquid interface, which can be useful in monitoring the stability of colloidal surfactants.

Finally, we experimentally confirmed the surfactant-like behavior of these amphiphilic Janus particles placed into mixtures of two immiscible liquids. Initially, the Janus particles were immersed into a mixture of heptane and water. From our initial experiments, we concluded that the particles were amphiphilic (i.e., they possess both hydrophobic and hydrophilic surface regions). For self-assembly, the particle geometry (e.g., shape, size, and size distribution) is an important factor that can influence the degree of self-organization at liquid–liquid interfaces. Thus, the shape of the bicompartmental PMMA particles was analyzed by SEM (Figure 2A). The SEM images confirm that EHD cojetting of bicompartmental PMMA solutions resulted in uniform spherical particles, albeit with a bimodal size distribution. A narrow size distribution and the uniform shapes of particles are believed to lead to more efficient organization of the surfactant-like particles at the interface.[39,40] Thus, we further refined the initial particle population by centrifugal separation. Centrifugation at 2000 rpm for 1 min resulted in two sets of particle samples having average particle diameters of 0.30 ± 0.04 μm and 2.19 ± 0.47 μm, respectively (Supporting Information Figure S1). A particle size of 300 nm was preferred, because smaller particles tend to be more efficient in preparing well-packed layers at liquid–liquid interfaces.[35] However, we still conducted the self-assembly study with the particles featuring an average diameter of 2 μm to ensure proper visualization of the compartments of individual particles at the interface by confocal laser scanning microscopy (CLSM). This is a prerequisite for confirming the orientation of the Janus particles at the liquid–liquid interface.

After initial agitation, the aqueous suspension of particles spontaneously self-assembled at the interface between the oil and water phases (Figure 5A, right). In order to confirm their equilibrium orientation, the bicompartmental particles were imaged by CLSM. As expected, the selected size range of the microparticles allowed for direct imaging of the orientation of the assembled particles. The compartments presenting polar hydroxyl groups were facing the aqueous phase, while the F-POSS-containing PMMA compartments pointed toward the heptane phase (Figure 5B and see Supporting Information Movie S1). Much like molecular surfactants, the amphiphilic Janus particles were minimizing the interfacial energy by self-organizing into two-dimensional colloidal sheets. The quantitative analysis of these images confirmed that more than 94% of the particles were selectively oriented at the interface (Supporting Information Figure S2). These results correlate well with the case, where the amphiphilic particles were incubated with hexadecane-in-water mixtures. Again, the stabilization of hexadecane droplets in water was promoted by the bicompartmental microparticles, as observed by CLSM imaging (Figure 5C). Due to their surfactant-like properties, the hydrophilic and hydrophobic compartments were fully exposed to either aqueous or oil phases, respectively. For

reference, isotropic particles that were composed of PMMA only preferred to locate in the water phase (Figure 5A, left).

3. CONCLUSION

Novel synthetic routes to fabricate amphiphilic Janus particles are needed for improved colloidal surfactants. Here, we have introduced an efficient approach to fabricate well-defined amphiphilic Janus particles by using our EHD cojetting method. This approach allows for fully decoupling the choice of materials used in two compartments of the same particle. Selective encapsulation of F-POSS in a first compartment significantly lowered the surface energy of one hemisphere. Concurrently, encapsulation and subsequent hydrolysis of PVAc in the second compartment increased the hydrophilicity of the second hemisphere, while maintaining their uniform size and shape. Moreover, successful integration of asymmetrical (i.e., polar and apolar) functionalities in each compartment was demonstrated by self-assembly of the obtained particles at a liquid−liquid interface. We believe this straightforward synthetic approach may constitute a significant contribution to future experimental studies as well as a number of different applications.

4. EXPERIMENTAL SECTION

Materials. Poly(methyl methacrylate) (PMMA, M_w = 120,000 g mol^{-1}), poly(vinyl acetate) (PVAc, M_w = 140,000 g mol^{-1}), sodium hydroxide, and N-(3-Dimethylaminopropyl)-N′-ethylcarbodiimide (EDC) were purchased from Sigma-Aldrich, U.S.A. N-Hydroxysulfosuccinimide (NHS) was purchased from Thermo Scientific, and rhodamine polyethylene glycol acid (RB-PEG-COOH, M_w = 3000 g mol^{-1}) was purchased from Nanocs, Inc., U.S.A. 1H,1H,2H,2H-Heptadecafluorodecyl polyhedral oligomeric silsequioxane (F-POSS) was synthesized as described elsewhere.[24,37] The fluorescence dyes poly[(m-phenylenevinylene)-*alt*-(2,5-dibutoxy-p-phenylenevinylene)] (MEHPV) and poly[tris(2,5-bis(hexyloxy)-1,4-henylenevinylene)-*alt*-(1,3-phenylenevinylene)] (PTDPV), which were used as CLSM markers with blue and green emission, were purchased from Sigma-Aldrich, U.S.A. The solvents tetrahydrofuran (THF), N,N′-dimethyl formamide (DMF), heptane, and hexadecane were purchased from Sigma-Aldrich, U.S.A. Asahiklin AK-225 (AK) was purchased from SPI Supplies, U.S.A. All solvents were used without further purification.

Preparation of PMMA Janus Particles. Two different polymer solutions were prepared in separate vials. Three w/v % of PMMA was dissolved in a solvent mixture of THF, DMF, and AK (50:45:5, v/v/v), and 0.3 w/v % (10% by weight of PMMA) of F-POSS was added to the solution. Another solution containing both, PMMA and PVAc (1:2, w/w), with a concentration of 3 w/v % of total weight of polymers, was prepared with the same ratio of solvents. The experimental setup contained a syringe pump (Fisher Scientific, Inc., U.S.A.), a power supply (DC voltage source, Gamma High Voltage Research, U.S.A.), and an aluminum foil as a flat collector. The two polymer solutions were delivered at a constant flow rate of 0.1 mL/h via vertically positioned syringes equipped with 26 G needles (Hamilton Company, U.S.A.). When a driving voltage of 6 kV was applied to the polymer solution, stable Taylor cone was formed and particles were collected at a distance of 40 cm. The temperature and humidity were maintained to 25 °C and 32%, respectively.

Surface Hydrolysis of Particles. A total volume of 4 mL of 0.01 M NaOH solution was added to 11 mL of the particle suspension (5.0 × 10^6 particles/ml), and the solution was stirred at 40 °C for 1 h for the surface hydrolysis of PVAc to PVA. After the reaction, the particles were washed with a centrifugal filter to remove excess NaOH until the pH of solution reached 7.

Rhodamine-labeled Particles by EDC/NHS Coupling. Surface hydrolysis of the particles was confirmed by conjugating dye molecules selectively on one side of the particles. The carboxyl groups of RB-PEG-COOH was activated with EDC and sulfo-NHS to form reactive NHS esters, and then covalently attached to the hydroxyl groups on the particle surface. Detailed reaction conditions are as follows. A volume of 950 μL of 10 mM RB-PEG-COOH/PBS with 0.01% Tween 20 was stirred with 40 mM EDC for 10 min, and then 10 mM NHS was incorporated into the solution for 10 min. Next, 50 μL of the particle suspension (5.0 × 10^7 particles/ml in 0.01% Tween 20/PBS) was reacted with the solution for 2 h. Finally, the particles were washed 20 times by centrifugation to remove any unreacted chemicals.

Fractionation of Particles. Once particles were collected from the jetting collector, it was required to fractionate the particles prior to their applications. Centrifugation allowed suspended particles to be separated into fractions of different sizes. The PMMA Janus particles were fractionated by centrifugation (Centrifuge 5810R, Eppendorf) at 2000 rpm for 1 min. The pellet had an average particle size of 2 μm, and was resuspended in a different vial (Supporting Information Figure S1A). The supernatant had an average particle size of 300 nm, as confirmed by DLS (Zetasizer Nano ZS, Malvern Instruments, U.K.), and was suspended separately (Supporting Information Figure S1B). The particle concentration of 5.0 × 10^7 particles/mL was measured by using particle analyzer (qNano, Izon).

Surface Energy Analysis. The substrates for surface energy analysis were prepared by spin-coating silicon wafers (2 cm long × 2 cm wide) with the desired polymer solution at 2000 rpm using a Specialty Coating Systems Spincoater G3P-8. The contact angle measurements were conducted using a Ramé-Hart 200-F1 goniometer. All the advancing contact angles reported in this work were measured by advancing a small volume of liquid (∼2 μL) onto the surface using a 2 mL micrometer syringe (Gilmont). At least three measurements were performed on each substrate.

Self-Assembly of Particles at Oil−Water Interfaces. A volume of 0.5 mL of particle suspension (5.0 × 10^7 particles/ml) and 0.5 mL of heptane were mixed by ultrasonication (Qsonica Q700, amplitude 10%) for 5 s for vigorous mixing of two liquids. In the case of the particles surrounding oil droplets in water, 5 μL of hexadecane were agitated with 0.5 mL of particle suspension and placed in a glass bottom well plate for 1 day. The particles at the interface of oil and water were imaged through z-stacks from CLSM and then three-dimensional (3D) reconstruction of the particles was made using Imaris software (Bitplane AG, Switzerland).

Quantitative Analysis of Selective Particle Orientation at the Interface. The orientation of each particle at the interface was analyzed from microscopic images for a total of four different samples using Matlab image processing software (The MathWorks, Inc., U.S.A.). 3D reconstructions of the particles taken from the interface were used for the analysis. Edges of blue and green domains were displayed and overlaid to calculate the average number of particles selectively oriented at the interface.

Particle Characterization. *ζ-Potential.* The ζ-potential of particles before and after the hydrolysis reaction were determined by using Zetasizer Nano ZS (Malvern Instrument, U.K.). All measurements were conducted in deionized water.

Fourier Transformed Infrared (FT-IR) Spectroscopy. The particle suspensions before and after the hydrolysis were deposited on Au-coated Si substrates and dried under vacuum for overnight. The measurements were performed on a Nicolet 6700 spectrometer utilizing the grazing angle accessory (Smart SAGA) at a grazing angle of 85°.

Scanning Electron Microscopy (SEM). The samples were coated with gold before analysis and the particle morphology was examined using an AMRAY 1910 field emission scanning electron microscope (FEG-SEM).

Confocal Laser Scanning Microscopy (CLSM). The particles were visualized using a CLSM (Olympus, FluoView 500). Three different lasers, 405 nm laser, 488 nm Argon laser, and 533 nm Helium−Neon green (HeNeG) laser, were used to excite the dyes MEHPV, PTDPV, and rhodamine groups of RB-PEG-COOH, respectively. The barrier filters were set to 430−460 nm for MEHPV, 505−525 nm for PTDPV, and 560−600 nm for RB-PEG-COOH.

■ ASSOCIATED CONTENT

Supporting Information

Fractionation of particles, quantitative analysis of particle orientations at water−oil interfaces. This material is available free of charge via the Internet at http://pubs.acs.org.

■ AUTHOR INFORMATION

Corresponding Author

*E-mail: lahann@umich.edu.

Notes

The authors declare no competing financial interest.

■ ACKNOWLEDGMENTS

The authors would like to acknowledge funding from the Multidisciplinary University Research Initiative of the Department of Defense (DOD) and the Army Research Office (W911NF-10-1-0518), the DOD through an idea award (W81XWH-11-1-0111), and from Dr. Charles Y.-C. Lee and the Air Force Office of Scientific Research (AFOSR) for financial support under grants FA9550-11-1-0017 and LRIR-12RZ03COR.

■ REFERENCES

(1) Teo, B. M.; Suh, S. K.; Hatton, T. A.; Ashokkumar, M.; Grieser, F. *Langmuir* **2011**, *27*, 30−33.

(2) Park, B. J.; Brugarolas, T.; Lee, D. *Soft Matter* **2011**, *7*, 6413−6417.

(3) Kim, S.-H.; Abbaspourrad, A.; Weitz, D. A. *J. Am. Chem. Soc.* **2011**, *133*, 5516−5524.

(4) Ding, S.; Zhang, C.; Wei, W.; Qu, X.; Liu, J.; Yang, Z. *Macromol. Rapid Commun.* **2009**, *30*, 475−480.

(5) Moon, J. J.; Huang, B.; Irvine, D. J. *Adv. Mater.* **2012**, *24*, 3724−3746.

(6) Misra, A. C.; Bhaskar, S.; Clay, N.; Lahann, J. *Adv. Mater.* **2012**, *24*, 3850−3856.

(7) Gangwal, S.; Pawar, A.; Kretzschmar, I.; Velev, O. D. *Soft Matter* **2010**, *6*, 1413−1418.

(8) Sotiriou, G. A.; Franco, D.; Poulikakos, D.; Ferrari, A. *ACS Nano* **2012**, *6*, 3888−3897.

(9) Pregibon, D. C.; Toner, M.; Doyle, P. S. *Science* **2007**, *315*, 1393−1396.

(10) Kim, S.-H.; Sim, J. Y.; Lim, J.-M.; Yang, S.-M. *Angew. Chem., Int. Ed.* **2010**, *49*, 3786−3790.

(11) Nisisako, T.; Torii, T.; Takahashi, T.; Takizawa, Y. *Adv. Mater.* **2006**, *18*, 1152−1156.

(12) Takahara, Y. K.; Ikeda, S.; Ishino, S.; Tachi, K.; Ikeue, K.; Sakata, T.; Hasegawa, T.; Mori, H.; Matsumura, M.; Ohtani, B. *J. Am. Chem. Soc.* **2005**, *127*, 6271−6275.

(13) Lv, W.; Lee, K. J.; Li, J.; Park, T.-H.; Hwang, S.; Hart, A. J.; Zhang, F.; Lahann, J. *Small* **2012**, *8*, 3116−3122.

(14) Faria, J.; Ruiz, M. P.; Resasco, D. E. *Adv. Synth. Catal.* **2010**, *352*, 2359−2364.

(15) Wang, Y.; Fan, D.; He, J.; Yang, Y. *Colloid Polym. Sci.* **2011**, *289*, 1885−1894.

(16) Tanaka, T.; Okayama, M.; Minami, H.; Okubo, M. *Langmuir* **2010**, *26*, 11732−11736.

(17) Meng, X.; Guan, Y.; Zhang, Z.; Qiu, D. *Langmuir* **2012**, *28*, 12472−12478.

(18) Binks, B. P.; Fletcher, P. D. I. *Langmuir* **2001**, *17*, 4708−4710.

(19) Ruhland, T. M.; Groschel, A. H.; Walther, A.; Müller, A. H. E. *Langmuir* **2011**, *27*, 9807−9814.

(20) Jiang, S.; Granick, S. In *Janus Particle Synthesis, Self-Assembly and Applications*; Jiang, S., Granick, S., Eds.; RSC Publishing: Cambridge, 2012; p 244.

(21) Roh, K.-H.; Martin, D. C.; Lahann, J. *Nat. Mater.* **2005**, *4*, 759−763.

(22) Bhaskar, S.; Lahann, J. *J. Am. Chem. Soc.* **2009**, *131*, 6650−6651.

(23) Lee, K. J.; Yoon, J.; Rahmani, S.; Hwang, S.; Bhaskar, S.; Mitragotri, S.; Lahann, J. *Proc. Nat. Acad. Sci. U.S.A.* **2012**, *109*, 16057−16062.

(24) Tuteja, A.; Choi, W.; Ma, M.; Mabry, J. M.; Mazzella, S. A.; Rutledge, G. C.; McKinley, G. H.; Cohen, R. E. *Science* **2007**, *318*, 1618−1622.

(25) Nuraje, N.; Khan, W. S.; Lei, Y.; Ceylan, M.; Asmatulu, R. *J. Mater. Chem. A* **2013**, *1*, 1929−1946.

(26) Lahann, J. *Small* **2011**, *7*, 1149−1156.

(27) Lee, K. J.; Hwang, S.; Yoon, J.; Bhaskar, S.; Park, T.-H.; Lahann, J. *Macromol. Rapid Commun.* **2011**, *32*, 431−437.

(28) Saha, S.; Copic, D.; Bhaskar, S.; Clay, N.; Donini, A.; Hart, A. J.; Lahann, J. *Angew. Chem., Int. Ed.* **2012**, *51*, 660−665.

(29) Wu, J.; Mather, P. T. *Polym. Rev.* **2009**, *49*, 25−63.

(30) Hosaka, N.; Otsuka, H.; Hino, M.; Takahara, A. *Langmuir* **2008**, *24*, 5766−5772.

(31) Yoon, J.; Lee, K. J.; Lahann, J. *J. Mater. Chem.* **2011**, *21*, 8502−8510.

(32) Bhaskar, S.; Hitt, J.; Chang, S.-W. L.; Lahann, J. *Angew. Chem., Int. Ed.* **2009**, *48*, 4589−4593.

(33) Roh, K. H.; Martin, D. C.; Lahann, J. *J. Am. Chem. Soc.* **2006**, *128* (21), 6796−6797.

(34) Bhaskar, S.; Pollock, K. M.; Yoshida, M.; Lahann, J. *Small* **2010**, *6*, 404−411.

(35) Owens, D. K.; Wendt, R. C. *J. Appl. Polym. Sci.* **1969**, *13*, 1741−1747.

(36) Young, T. *Philos. Trans. R. Soc. London* **1805**, *95*, 65−87.

(37) Meuler, A. J.; Chhatre, S. S.; Nieves, A. R.; Mabry, J. M.; Cohen, R. E.; McKinley, G. H. *Soft Matter* **2011**, *7*, 10122−10134.

(38) Aveyard, R.; Binks, B. P.; Clint, J. H. *Adv. Colloid Interface Sci.* **2003**, *100−102*, 503−546.

(39) Hunter, T. N.; Pugh, R. J.; Franks, G. V.; Jameson, G. J. *Adv. Colloid Interface Sci.* **2008**, *137*, 57−81.

(40) Mabry, J. M.; Vij, A.; Iacono, S. T.; Viers, B. D. *Angew. Chem., Int. Ed.* **2008**, *47*, 4137−4140.